Soft Matter

Cite this: *Soft Matter*, 2011, **7**, 6678

www.rsc.org/softmatter

PAPER

Chain formation in a magnetic fluid under the influence of strong external magnetic fields studied by small angle neutron scattering

Matthew Barrett,[a] Andreas Deschner,[a] Jan P. Embs[b] and Maikel C. Rheinstädter*[ac]

Received 20th January 2011, Accepted 21st April 2011
DOI: 10.1039/c1sm05104k

We studied the aggregation of magnetic particles into chain-like structures in a cobalt-based magnetic fluid, exposed to external magnetic fields. The length of chain segments in very strong magnetic fields of up to 2 Tesla was measured *in situ* using small angle neutron scattering. Arrangement of the magnetic particles was studied with the scattering vector $\vec{Q}$ aligned parallel to the magnetic field lines, and at angles of 30° and 60° with respect to $\vec{B}$. Although chains several hundred particles in length were predicted, we observe a maximum correlation length of ~65 nm equivalent to 3–4 particles up to highest fields. We speculate that the interaction between chains, *i.e.*, the interplay between the entropy and energy of the system combined with the particular properties of the magnetic dipole–dipole interaction ultimately decide the length of the particle chains.

I. Introduction

Magnetic model systems are usually studied using ferromagnetic and antiferromagnetic Heisenberg, XY and Ising type interactions of different dimensionality.[1] In contrast to magnetic lattices, which are realized in magnetic crystals, magnetic fluids behave like highly permeable paramagnetic gases. Here, magnetic particles interact *via* long-range dipole–dipole interactions rather than short-range direct magnetic interactions. The magnetic fluid's macroscopic properties, such as a magnetic field dependent viscosity, are strongly determined by the magnetism of the embedded nanoparticles. These so-called "ferrofluids" are colloidal suspensions of nanodomain particles with a typical magnetic core diameter of $\sigma \sim 10$ nm in a liquid carrier,[2] see ref. 3 for a recent review. Magnetic relaxation is dominated by two distinct mechanisms. First, Néel relaxation, which describes the reorientation of the magnetic moment of a particle relative to its stationary magnetic core. Second, Brownian relaxation, in which the magnetic moment is tightly fixed to each particle, takes place *via* rotation of the whole particle relative to the fluid. For sufficiently large particles, the Brownian mechanism prevails as the Néel relaxation time becomes infinitely long.[4] The unique macroscopic properties of such a magnetic fluid are determined by the interactions between the giant magnetic moments of the particles (some ten thousand μ_B) and the presence of an external magnetic field, $\vec{B}$. In particular Small Angle Neutron Scattering (SANS) has proven to be a useful tool to investigate the microstructure of ferrofluids. Particle size distribution, interparticle interactions, phase diagrams and structure formation with and without an external magnetic field have been studied using this technique.[5–14]

In a magnetic fluid the magnetic cores are nanometre sized, single domain particles, usually made of magnetite, Fe_3O_4, or cobalt. To avoid agglomeration, these grains are coated by a polymeric layer, as is depicted in Fig. 1a. Ferrofluids are

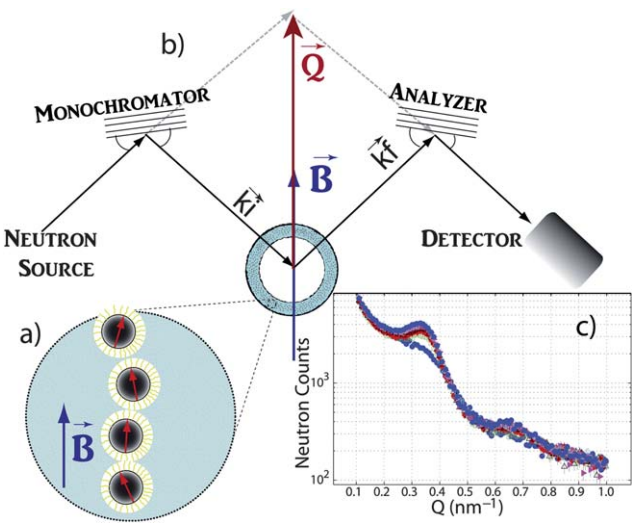

Fig. 1 (Colour online). a) Chain formation of magnetic particles. Cobalt cores (represented in black) each possess a thin polymer coating (represented in yellow). The magnetic moment is represented by an arrow. b) Schematic diagram of the experimental setup, with the magnetic field aligned parallel to the scattering vector, $\vec{Q}$. c) Small angle neutron scattering data for different magnetic field strengths.

[a]*Department of Physics and Astronomy, McMaster University, Hamilton, ON, Canada. E-mail: rheinstadter@mcmaster.ca*
[b]*Laboratory for Neutron Scattering, ETH Zürich & Paul Scherrer Institut, 5232 Villigen, PSI, Switzerland*
[c]*Canadian Neutron Beam Centre, National Research Council Canada, Chalk River, ON, Canada*

macroscopically superparamagnetic ($\mu \approx 1$), with a viscosity which can be tuned continuously using an applied magnetic field by the magnetoviscous effect.[3,15] In magnetite based ferrofluids, magnetic moments of about $10^4\ \mu_B$ were reported ($\mu_B = e\hbar/(2m_e) = 9.27 \times 10^{-24}$ J T^{-1}). They are well described by inclusion of magnetic terms in the Navier–Stokes equation[2] and their behavior is influenced by both hydrodynamics as well as magnetism (sometimes called magnetohydrodynamics). Alternatively, cobalt based magnetic fluids have larger magnetic moments of up to $8 \times 10^4\ \mu_B$, and their behavior is primarily determined by magnetic interactions, *i.e.* the interaction of a magnetic dipole with the external magnetic field and neighbouring magnetic particles. The potential energy, u, of a particle i can be written as:

$$u_i = -\vec{m}_i \cdot \vec{B} + \sum_j -\vec{m}_i \cdot \frac{\mu_o}{4\pi r_{ij}^3}\{3(\vec{m}_j \cdot \hat{r}_{ij})\hat{r}_{ij} - \vec{m}_j\}, \qquad (1)$$

with $m_{i,j}$ the magnetic moments of the particles, $\vec{B}$ the external magnetic field and $\mu_0 = 4\pi \times 10^{-7}$ N A^{-2}. The influence of particle interaction on the physical properties of the ferrofluid mainly depends on two parameters, the volume fraction of the particles, ϕ, and the dipolar coupling constant, λ. ϕ is given by $\phi = \frac{N}{V}\frac{\pi\sigma^3}{6}$, with σ the particle diameter. The dipolar coupling constant relates the dipole–dipole interaction energy of two contacting particles to the thermal energy k_BT, with k_B the Boltzmann constant (1.38×10^{-23} J K^{-1}) and T the absolute temperature. λ is defined as:

$$\lambda = \frac{m^2}{4\pi\mu_0 k_B T \sigma^3}. \qquad (2)$$

While λ in magnetite based ferrofluids is found to be $\lambda \sim 0.3$ at room temperature, the dipolar coupling in cobalt based ferrofluids is about two orders of magnitude stronger with λ values of up to $\lambda = 20$. For the magnetic fluid used in this study, we determined $\lambda = 18$. Because of the dominant magnetic dipole–dipole interaction cobalt based magnetic fluids are prime model systems to study fundamental properties in magnetic fluids, such as structure formation.

To explain certain magnetic properties, such as the large susceptibility, it was speculated that magnetic particles aggregate into larger structures, which show cooperative magnetic behaviour. Theoretical investigations started with de Gennes and Pincus,[16] later followed by Jordan.[17] In these works the ferrofluid is modeled as a monodisperse fluid of hard spheres of diameter σ, carrying central point dipoles of magnitude m. One-dimensional chains oriented along the field lines of an applied magnetic field, were predicted.[18,19] The length of these chains was speculated to be a monotonically increasing function of an external magnetic field. Long chains were also observed in Monte Carlo simulations of monodisperse ferrofluids.[20] Aggregation and structure formation have been studied and chain formation was observed with transmission electron microscopes (TEM) in freeze dried 2d films of magnetite based ferrofluids[21,22] and in both, polarized and non-polarized small angle neutron scattering with magnetic fields in the order of 0.01–0.2 T.[23–25] Small and moderate magnetic fields have been used to measure susceptibility and magnetization in standard laboratory experiments. For these field strengths the dipole–field interaction is comparable to thermal energies. In large external fields, however, the dipole–external field interaction should become the dominant term in eqn (1) and lead to the formation of long one-dimensional chains parallel to the magnetic field lines.[16,18,19] However, from *in situ* neutron diffraction experiments at room temperature, in the fluid state of the magnetic fluid, we find that the chain length saturates in large external magnetic fields of up to 2 T for chain segments of about 4 particles. This behavior can be speculated to be the result of the interaction between chain segments and stems from the competition between magnetic energy, the entropy of the nanoparticles and the peculiar properties of the dipole–dipole interaction of the giant magnetic moments, as will be discussed below.

II. Experiment

To study the aggregation of magnetic particles, we investigated a magnetic fluid composed of cobalt particles. The fluid was provided by Kardiotechnik, Berlin. The Co particles were coated by lauryol-sarcosine and dispersed in a diffusion pump oil (Edwards L9). A thickener agent consisting of either polyisobutylene-succinimide or Lubrizol 7761A was added to enhance the viscosity of the sample. Ferrofluids can be characterized by a number of techniques to determine the size of the magnetic core, thickness of the nonmagnetic layer as well as particle size distribution.[26–28] The investigated ferrofluid has been characterized using magneto-granulometry (MG), photon correlation spectroscopy (PCS) and torsional-pendulum (TP) measurements.[29–32] Values for the core-size D_o, polydispersity parameter σ, saturation magnetization M_s, the volume averaged core-diameter D_v and volume weighted core-diameter D_{vol} are listed in Table 1.

From measurements of the saturation magnetization, the volume fraction of cobalt in the undiluted samples was determined to be $\varphi = 1.5\%$. From this result, we determined the volume fraction of the whole particle (including both the cobalt core and polymer coating) to be $\varphi = 8.75\%$. The dynamic fluid viscosity was determined as $\eta = 0.5$ Pa s. From the values in Table 1 the thickness of the surfactant coating can be estimated to (2.5 ± 1.0) nm. This value takes into account the fact that different measurement techniques have access to different diameters; the TP as well as the PCS method are sensitive to the hydrodynamic diameter of the particles, whereas with MG the magnetic diameter is probed. In addition to this magnetic diameter, the particles show up with a so called magnetic dead layer close to the particle's surface.

Table 1 Values for the core-size D_o, polydispersity parameter σ, saturation magnetization M_s, the volume averaged core-diameter D_v and volume weighted core-diameter D_{vol}, as taken from ref. 31

Cobalt Ferrofluid	MG	PCS	TP
D_o (nm)	11.0	19.0	—
σ (nm)	1.27	1.2	—
M_s (A m^{-1})	6512	—	—
D_v (nm)	12.0	20	—
D_{vol} (nm)	13.5	22	16.2

Furthermore one has to keep in mind that the methods mentioned above are sensitive to different moments of the underlying particle size distribution; this point and its consequences are discussed in great detail in ref. 30–32.

The neutron diffraction experiments were conducted on the cold triple-axis spectrometer IN12 at the Institut Laue-Langevin in Grenoble, France. To avoid Bragg peaks from the sample container a double walled cylindrical vanadium sample can with an outside diameter of 10 mm, an inside diameter of 9 mm and a length of 60 mm was used. About 1.5 millilitres of ferrofluid was filled in the 1 mm space between inner and outer cylinder, as sketched in Fig. 1b. Note that the carrier fluid is a strong incoherent scatterer with correspondingly strong absorption. Geometry and volume of the can were designed to optimize scattering and minimize absorption of the ferrofluid. We calculated the magnetic field distribution for this set-up. As the ferrofluid used is superparamagnetic $\mu \approx 1$ the field inside the sample container does not distort with respect to the external field. We note that the vanadium walls of the cylinder lead to a slight attenuation of the magnetic field inside our sample container. We estimate this shielding effect to be less than 5%, as the thickness of the wall was less than 1/10th of a millimetre. This can was installed into a 4 T horizontal field cryomagnet. A neutron wavelength of 0.418 nm was used and the collimation was set to 35′-monochromator-10′-sample-10′-analyzer-30′-detector, resulting in an instrumental resolution of $\Delta Q = 0.06$ nm^{-1}. All experiments were conducted at room temperature, at $T = 293$ K. Small angle neutron scattering (SANS) was then measured in the presence of magnetic fields of up to 2 T. Due to the torque created by the large external magnetic field on our fluid, it was not possible to measure at higher fields. Preliminary tests have shown that the carrier fluid and polymer shells result in a high incoherent background, which makes it difficult to detect the small coherent correlation peaks. On a triple-axis spectrometer the analyzer cuts out only the elastically scattered neutrons. The quasi-elastic contributions of the protons to the background are omitted, reducing the background and improving the signal to noise ratio drastically. The combination of a low background, good Q-resolution, the use of an analyzer, and the option for a powerful horizontal magnet made IN12 highly suited for these measurements.

The static structure factor $S(Q)$ was determined in external magnetic fields of 0, 0.1, 0.25, 0.5, 1.0, 1.5, and 2 Tesla. We note, however, that at $B = 0$ T there was a remnant field due to hysteresis effects of the setup, which we estimate to be ~0.01 T. The scattering vector $\vec{Q}$ was placed parallel to the magnetic field lines, and at angles of 30° and 60°. Small angle scattering data are shown in Fig. 1c. To display only contributions from the coherent inter particle scattering, a q^{-4} background was subtracted from the data. The results are shown in Fig. 2 for $B = 0.1$ T and $B = 2$ T. The scans exhibit a pronounced correlation (Bragg) peak at ~ 0.34 nm^{-1}, corresponding to a particle–particle distance of ~18.5 nm. Assuming that the particles are in contact with each other, the particle size σ should be equivalent to the inter particle distance. This value is in good agreement with size determination by other techniques[29–32] and suggests that the polymer shells of the particles are in direct contact. A weak second order peak is visible in the data at higher magnetic fields,

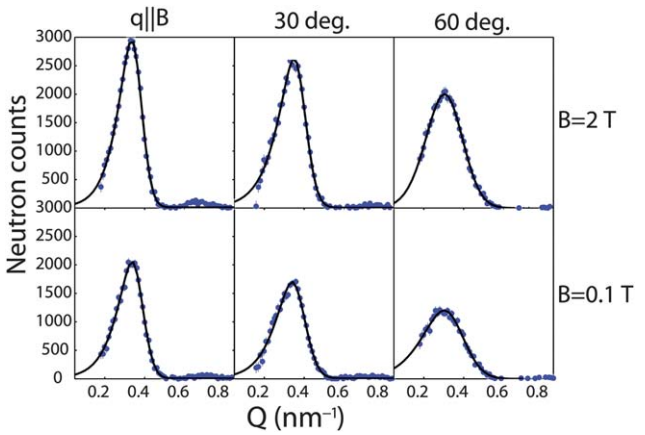

Fig. 2 (Colour online). Data at B-field strengths of 2 T (top row) and 0.1 T (bottom row) and at angles formed by the $\vec{Q}$-vector and $\vec{B}$-field, parallel, 30°, 60° (left to right). The solid lines are fits using an asymmetric Gaussian peak profile, as described in the text.

pointing to increased order, possibly due to the suppression of thermal fluctuations in the particles. The asymmetry of the peaks reflects the particle size distribution, which is well described by a log-normal distribution.[29–32] To fit the diffraction data we modified an Exponential-Gaussian hybrid function.[33] This asymmetric peak shape takes into account the asymmetry of the particle size distribution, convoluted with the Gaussian resolution of the spectrometer.

$$f_{\mathrm{egh}}(Q) = H(Q_0 - Q)\cdot A\exp\left(\frac{-(Q-Q_0)^2}{2\sigma_g^2 + \tau(Q-Q_0)}\right) + H(Q-Q_0)\cdot A\exp\left(\frac{-(Q-Q_0)^2}{2\sigma_g^2}\right) \quad (3)$$

with σ_g the Gaussian width, Q_0 the peak position, A as the amplitude, τ the asymmetry parameter and $H(x)$ the Heaviside step function.

The particle–particle distance, number and length of the corresponding chain segments could then be determined from position, amplitude and width of the correlation peak. Amplitude, peak width and position of the Bragg peaks for varying angles between $\vec{Q}$ and $\vec{B}$, as determined from the fits of the elastically scattered neutron data in Fig. 2, are depicted in Fig. 3. Some trends are visible: the intensity of the peaks increases with increasing field, and the peak widths are narrow in the direction of the magnetic field lines and become wider with increasing angle. As the peak intensity is proportional to the number of chain segments, this points to an increasing number of aggregates. The data in Fig. 3 strongly depend on the angle between scattering vector and applied magnetic field. The shape of the conglomerate is strongly anisotropic: it is elongated along the magnetic field lines as the peak width drastically increases with increasing angle. The width decreases as a function of the external field until about 0.25 T for all angles and stays constant for stronger fields. The position of the correlation peak shifts to larger Q values with increasing magnetic field, which points to a slightly decreasing inter particle distance at stronger fields, possibly due to the suppression of thermal fluctuations of the particles.

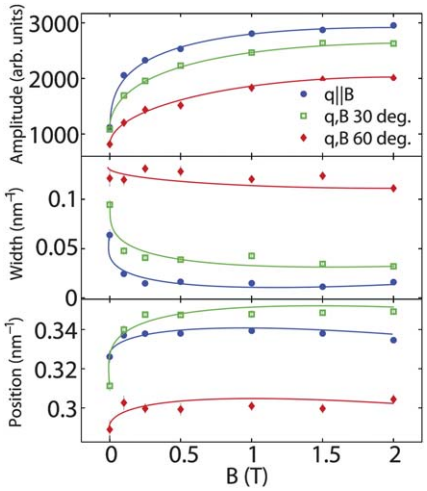

Fig. 3 (Colour online). Amplitude, peak width and position of the Bragg peak for angles of 0, 30 and 60° between $\vec{Q}$ and $\vec{B}$, as determined from the fits of the elastically scattered neutron data in Fig. 2. (Solid lines are guides to the eye.)

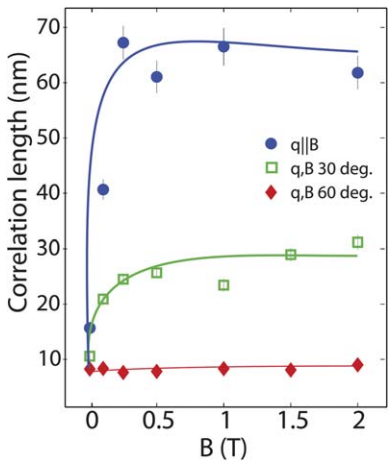

Fig. 4 (Colour online). Correlation length, ξ, at angles of 0, 30, and 60° between $\vec{Q}$ and $\vec{B}$. The correlation length for all angles shows a steep increase at small fields and saturates at high fields. (Solid lines are guides to the eye.)

Fig. 4 depicts the correlation length, calculated as $\xi = 1/\text{width}$, as a function of magnetic field. The correlation length parallel to the field lines, $\xi_{\|}$, shows a steep increase up to fields of about 0.25 T. The length of the chain segments then saturates for high fields at values of about 65 nm, which corresponds to chains between 3 and 4 particles (3.5 particles). The correlation length measured at 30° also increases at small fields to saturate at values of $\xi_{30} \sim 30$ nm. ξ_{60} appears to be constant at values of $\xi_{60} \sim 9$ nm, half a particle diameter.

III. Discussion

From the existence of pronounced Bragg peaks in the diffraction data in Fig. 2 we can conclude that the particles form aggregates. By varying the angle between the applied external magnetic field and momentum transfer vector we find evidence that these aggregates are strongly anisotropic and most likely resemble chain-like structures, oriented along the applied magnetic field lines. The value for σ is in good agreement with theoretical predictions and experimental observations reported by other techniques.[21–25] The amplitude, width and position of the observed Bragg peaks in Fig. 3, as a function of the external field, have a high rate of change for fields of about 0.25 T and saturate at higher magnetic fields. The area of the correlation peaks in Fig. 3a can be considered to be proportional to the number of chain segments in the system. With increasing magnetic field strength, we find that more chain segments form.

The correlation length parallel to the magnetic field lines, $\xi_{\|}$, as shown in Fig. 4, shows values of slightly less than ~18 nm at the smallest field, less than the distance between two particles. Note that our scattering experiment is not sensitive to the existence of monomers as single particles do not contribute to Bragg scattering. At low fields the fluid, therefore, most likely consists of a mixture of monomers and pairs of particles, so-called dimers. The axes of the dimers, however, are not well aligned along the external field as a result of the competition between dipole–dipole and dipole–field interaction. The projection along the field lines is then smaller than the particle distance. A possible structure of the magnetic fluid at small fields is sketched in Fig. 5a. $\xi_{\|}$ then saturates with higher fields, at values of ~65 nm,

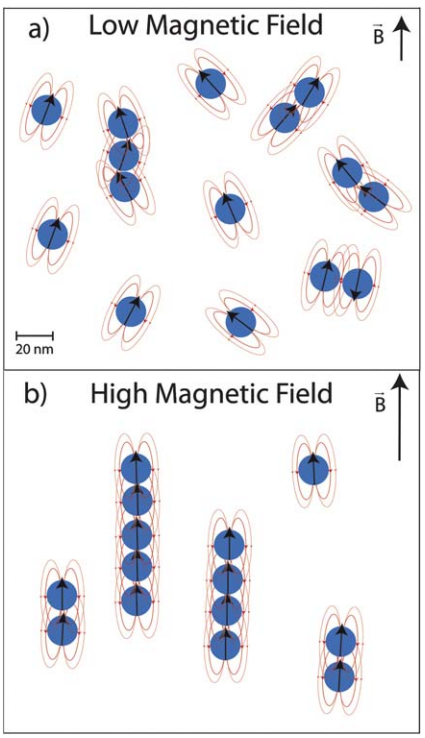

Fig. 5 (Colour online). Particle distribution, as suggested by the experimental data, at low and high field. In the small field case (a), the dipole–dipole interaction is comparable in magnitude to the dipole–field interaction, resulting in short, kinked chains. In the large field case (b), all magnetic moments are aligned parallel to the magnetic field lines resulting in well aligned chains. Depending on their relative position, chain segments can repel one another, making it difficult to form longer chains.

corresponding to an average chain length of 3.5 particles, as sketched in Fig. 5b. The dipole–field interaction term in eqn (1) is now dominant and all magnetic moments are perfectly aligned to the external field. As a result, the chains forming are well oriented along the field lines. Thermal fluctuations are suppressed as evidenced by the slightly decreasing inter-particle distance and the occurrence of higher order Bragg reflections as seen in Fig. 2. The chain length, however, seems to saturate at short chain segments. This experimental finding is in contrast to theoretical predictions of chain lengths increasing monotonically, with external magnetic fields.[16–20] While monodisperse systems were investigated in these studies, the effect of polydisperisity has also been studied.[34–36] It was found that a distribution of particle sizes may reduce the chain length. As smaller particles can be expected to have weaker interaction, the occurrence of large and small particles in a chain was speculated to induce stronger and weaker particle–particle bonds. Due to the variation in particle distribution, long chains may more easily break where two small particles are in contact with one another.

The lengths of the chain segments observed in this experiment are also shorter than the chain lengths reported from cryo-TEM experiments in vitrified 2d films of synthetic magnetite based ferrofluids. The occurrence of relatively short chain-segments in the cobalt based ferrofluid may be the result of strong external fields in combination with the large magnetic moments of the particles and the peculiar geometry of the dipole–dipole interaction. In strong external fields, all the spins should be aligned parallel to the external field. Pairs or short segments form first in low magnetic fields. To combine short chains into longer chains, segments must approach one another with appropriate directional orientation. If two chains approach head-to-tail there is an attractive interaction, which might lead to the formation of longer chains. Alternatively, segments which approach from the side experience a repulsive force because of the shape of the magnetic field lines; as pictured in Fig. 5. The magnetic field of a 1d chain is proportional to the number of particles in the chain. The magnetic dipole field lines, however, condense more closely around the chain as the chain length increases (compare Fig. 5 a and b). This can lead to the peculiar situation that long chain segments do not "feel" each other over large distances. They may, however, experience a strong repulsive interaction if they approach each other laterally. As has been speculated previously,[37] the strong inter-chain interaction therefore most likely prevents the formation of long chains. We note that our observation of relatively short chain segments agrees qualitatively with molecular dynamics simulations[38] and mean-field theories.[39] The formation of short chain segments was recently also reported from Langevin dynamics computer simulations,[40] in very good agreement to the values reported here.

The particular properties of magnetic fluids in a magnetic field, such as the tunable viscosity can at least partially be attributed to the repulsive interactions between relatively short chain segments. The situation is probably different in magnetite based ferrofluids with much weaker dipole–dipole interactions. Here longer chains may form because the repulsive force can possibly be overcome by thermal fluctuations more easily. Our experimental setup will be used in future experiments to study chain formation in magnetite based fluids. Longer chains are expected at strong magnetic fields as the inter-chain interaction is smaller when compared to the cobalt based fluid studied here.

IV. Conclusion

In summary, we have studied chain formation of magnetic particles in a cobalt based magnetic fluid in strong external magnetic fields of up to 2 T. In contrast to previous experiments and theoretical predictions, we observe relatively short chain segments of 3–4 particles. We speculate that the strong inter-chain interaction and the geometry of the magnetic dipole–dipole interaction prevent the formation of longer chains.

Acknowledgements

This research was partially funded by the Natural Sciences and Engineering Research Council of Canada (NSERC) and the National Research Council of Canada (NRC). We thank the Jülich Centre for Neutron Science (JCNS) and the Institut Laue Langevin for the allocation of beam time. We thank N. Buske (Kardiotechnik, Berlin) for providing the Cobalt-based ferrofluid.

References

1 L. de Jongh and A. Miedema, *Adv. Phys.*, 2001, **50**, 947.
2 R. Rosensweig, *Ferrohydrodynamics* (Cambridge University Press, England, 1985).
3 S. Odenbach, ed., *Colloidal Magnetic Fluids: Basics, Development and Application of Ferrofluids* (Springer, Heidelberg, 2009).
4 M. Shliomis, *Sov. Phys. Usp.*, 1974, **17**, 153.
5 D. Cebula, S. Charles and J. Popplewell, *J. Magn. Magn. Mater.*, 1983, **39**, 67.
6 R. Rosman, J. Janssen and M. Rekveldt, *J. Appl. Phys.*, 1990, **67**, 3072.
7 F. Boue, V. Cabuil, J. Bacri and R. Perzynski, *J. Magn. Magn. Mater.*, 1993, **122**, 78.
8 R. Mehta, P. Goyal, B. Dasannacharya, R. Upadhyay, V. Aswal and G. Sutariya, *J. Magn. Magn. Mater.*, 1995, **149**, 47.
9 E. Dubois, R. Perzynski, F. Boue and V. Cabuil, *Langmuir*, 2000, **16**, 5617.
10 G. Meriguet, E. Dubois, A. Bourdon, G. Demouchy, V. Dupuis and R. Perzynski, *J. Magn. Magn. Mater.*, 2005, **289**, 39.
11 C. Neto, M. Bonini and P. Baglioni, *Colloids Surf., A*, 2005, **269**, 96.
12 L. Pop and S. Odenbach, *J. Phys.: Condens. Matter*, 2006, **18**, S2785.
13 M. Klokkenburg, B. Erne, A. Wiedenmann, A. Petukhov and A. Philipse, *Phys. Rev. E: Stat., Nonlinear, Soft Matter Phys.*, 2007, **75**, 051408.
14 D. Bica, L. Vekas, M. Avdeev, O. Marinica, V. Socoliuc, M. Balasoiu and V. Garamus, *J. Magn. Magn. Mater.*, 2007, **311**, 17.
15 S. Odenbach, *J. Phys.: Condens. Matter*, 2004, **16**, R1135.
16 P. G. de Gennes and P. A. Pincus, *Eur. Phys. J. B*, 1970, **11**, 189.
17 P. Jordan, *Mol. Phys.*, 1973, **25**, 961.
18 K. Morozov and A. Lebedev, *J. Magn. Magn. Mater.*, 1990, **85**, 51.
19 V. S. Mendelev and A. O. Ivanov, *Phys. Rev. E: Stat., Nonlinear, Soft Matter Phys.*, 2004, **70**, 051502.
20 P. J. Camp and G. N. Patey, *Phys. Rev. E: Stat. Phys., Plasmas, Fluids, Relat. Interdiscip. Top.*, 2000, **62**, 5403.
21 M. Klokkenburg, R. P. A. Dullens, W. K. Kegel, B. H. Erné and A. P. Philipse, *Phys. Rev. Lett.*, 2006, **96**, 037203.
22 M. Klokkenburg, B. H. Erné, J. D. Meeldijk, A. W. A. V. Petukhov, R. P. A. Dullens and A. P. Philipse, *Phys. Rev. Lett.*, 2006, **97**, 185702.
23 A. Wiedenmann, U. Keiderling, M. Meissner, D. Wallacher, R. Gähler, R. May, S. Prévost, M. Klokkenburg, B. Erné and J. Kohlbrecher, *Phys. Rev. B: Condens. Matter Mater. Phys.*, 2008, **77**, 184417.
24 A. Wiedenmann and A. Heinemann, *J. Magn. Magn. Mater.*, 2005, **289**, 58.

25 A. Wiedenmann, A. Hoell and M. Kammel, *J. Magn. Magn. Mater.*, 2002, **252**, 83.
26 A. Ivanov and S. Kantorovich, *Phys. Rev. E*, 2004, **70**, 021401.
27 C. Holm, A. Ivanov, S. Kantorovich, E. Pyanzina and E. Reznikov, *J. Phys.: Condens. Matter*, 2006, **18**, S2737.
28 Z. Wang and C. Holm, *Phys. Rev. E*, 2003, **68**, 041401.
29 J. Embs, S. May, C. Wagner, A. Kityk, A. Leschhorn and M. Lücke, *Phys. Rev. E: Stat., Nonlinear, Soft Matter Phys.*, 2006, **73**, 036302.
30 J. P. Embs, B. Huke, A. Leschhorn and M. Lücke, *Z. Phys. Chem.*, 2008, **222**, 527586.
31 J. Embs, H. W. Müller, C. E. K. III, F. Meyer, H. Natter, B. Müller, S. Wiegand, M. Lücke, K. Knorr and R. Hempelmann, *Z. Phys. Chem.*, 2006, **220**, 153.
32 J. Embs, H. Müller, M. Lücke and K. Knorr, *Magnetohydrodynamics*, 2000, **36**, 320.
33 K. Lan, *J. Chromatogr., A*, 2001, **915**, 1.
34 E. Pyanzina, S. Kantorovich, J. Cerda, A. Ivanov and C. Holm, *Phys. Rev. E*, 2009, **107**, 571.
35 J. Cerda, E. Elfimova, V. Ballenegger, E. Krutikova, A. Ivanov and C. Holm, *Phys. Rev. E: Stat., Nonlinear, Soft Matter Phys.*, 2010, **81**, 011501.
36 J. Huang, Z. Wang and C. Holm, *Phys. Rev. E*, 2005, **71**, 061203.
37 L. Y. Iskakova and A. Y. Zubarev, *Phys. Rev. E: Stat. Phys., Plasmas, Fluids, Relat. Interdiscip. Top.*, 2002, **66**, 041405.
38 Z. Wang, C. Holm and H. W. Müller, *Phys. Rev. E: Stat. Phys., Plasmas, Fluids, Relat. Interdiscip. Top.*, 2002, **66**, 021405.
39 A. O. Ivanov, Z. Wang and C. Holm, *Phys. Rev. E: Stat., Nonlinear, Soft Matter Phys.*, 2004, **69**, 031206.
40 J. S. Andreu, J. Camachob and J. Faraudo, *Soft Matter*, 2011, **7**, 2336.